Journal of Photochemistry and Photobiology A: Chemistry 207 (2009) 109–114

Contents lists available at ScienceDirect

Journal of Photochemistry and Photobiology A: Chemistry

journal homepage: www.elsevier.com/locate/jphotochem

Architecture of supramolecular metal complexes for photocatalytic CO_2 reduction III: Effects of length of alkyl chain connecting photosensitizer to catalyst

Kazuhide Koike [a], Sayoko Naito [b], Shunsuke Sato [b], Yusuke Tamaki [b], Osamu Ishitani [b,c,*]

[a] National Institute of Advanced Industrial Science and Technology, Onogawa 16-1, Tsukuba 305-8569, Japan
[b] Department of Chemistry, Graduate School of Science and Engineering, Tokyo Institute of Technology, O-okayama 2-12-1, E1-9, Meguro-ku, Tokyo 152-8551, Japan
[c] SORST, JST, Honmati 4-1-8, Kawaguti, Saitama 332-0012, Japan

ARTICLE INFO

Article history:
Available online 24 December 2008

This paper is dedicated to Professor Haruo Inoue's 60th birthday.

Keywords:
Photocatalyst
CO_2 reduction
Supramolecule
Metal complex

ABSTRACT

New Ru(II)–Re(I) binuclear complexes $[\{Ru(dmb)_2\}\text{-LL-}\{Re(CO)_3Cl\}]^{2+}$(dmb = 4,4′-dimethyl-2,2′-bipyridine) with 1,2-bis(4′-methyl-[2,2′]bipyridinyl-4-yl)-ethane (**MebpyC$_2$H$_4$Mebpy**), 1,4-bis(4′-methyl-[2,2′]bipyridinyl-4-yl)-butane (**MebpyC$_4$H$_8$Mebpy**), and 1,6-bis(4′-methyl-[2,2′]bipyridinyl-4-yl)-hexane (**MebpyC$_6$H$_{12}$Mebpy**) as bridge ligands (LL) have been synthesized, and their photocatalytic activity for CO_2 reduction has been investigated. The most efficient photocatalyst had **MebpyC$_2$H$_4$Mebpy** as the bridge ligand, but no difference in photocatalysis was observed between the diads with **MebpyC$_4$H$_8$Mebpy** and **MebpyC$_6$H$_{12}$Mebpy**. Weak interaction between the Ru and Re sites was observed only through the **MebpyC$_2$H$_4$Mebpy** ligand but not through the other bridge ligands. This interaction induces a higher reductive quenching efficiency of the ^{3}MLCT excited state of the diad with **MebpyC$_2$H$_4$Mebpy** by the reductant, BNAH, and consequently the quantum yield of CO_2 reduction is higher.

1. Introduction

The photochemical utilization of CO_2 with solar energy is a promising candidate for addressing both the shortage of fossil fuels and the global warming problem. Rhenium(I) bipyridine tricarbonyl complexes can function as both photocatalysts and electrocatalysts for CO_2 reduction [1–6]. Although their efficiencies and product selectivities are quite high, in order to achieve the efficient use of solar light, a photosensitizer, which effectively drives photochemical electron transfer with visible light, must cooperate with a rhenium complex catalyst, which cannot absorb a wide range of visible light.

We have reported that a novel type of supramolecular photocatalysts with both ruthenium(II) and rhenium(I) complexes linked by 1,3-bis(4′-methyl-[2,2′]bipyridinyl-4-yl)-propan-2-ol (bpyC3(OH)bpy), such as **RuC3(OH)Re** (Scheme 1), work well as photocatalysts for CO_2 reduction [7,8]. The photocatalytic activities of these diads are much higher than the corresponding mixed systems with mononuclear Ru and Re complexes. One of the most important findings is that the two diimine regions of the bridge ligand, which each coordinate to Ru(II) or Re(I), should not be conjugated because the conjugation lowers the energy level of the π^* orbital of the diimine, which lower the reduction ability of the Re(I) complex [7].

It is reasonable to expect that the distance between the Ru(II) and Re(I) units is another important factor affecting photocatalysis, because electron transfer must occur between these units during CO_2 reduction. We now report syntheses of new Ru(II)-Re(I) diads **RuCnRe** with different lengths of a alkyl chains as bridging ligands, as shown in Scheme 1, and the effects of chain length on the photophysical and electrochemical properties of the diads. Additionally, we report the photocatalytic competencies of the diads.

2. Results and discussion

2.1. Photophysical properties

Fig. 1 shows the UV–vis absorption spectra of **RuC2Re** with those of the corresponding Ru(II) and Re(I) mononuclear complexes. All spectra of the diads were very similar to each other and were almost consistent with the 1:1 summation spectrum of the mononuclear complexes. These results clearly indicate that there is no strong interaction between the Ru(II) and Re(I). Because of this, the absorption bands at 320–450 and 400–500 nm can be assigned to MLCT

* Corresponding author at: Department of Chemistry, Graduate School of Science and Engineering, Tokyo Institute of Technology, O-okayama 2-12-1, E1-9, Meguro-ku, Tokyo 152-8551, Japan. Tel.: +81 3 5734 2240; fax: +81 3 5734 2240.
E-mail address: ishitani@chem.titech.ac.jp (O. Ishitani).

1010-6030/$ – see front matter © 2008 Elsevier B.V. All rights reserved.
doi:10.1016/j.jphotochem.2008.12.014

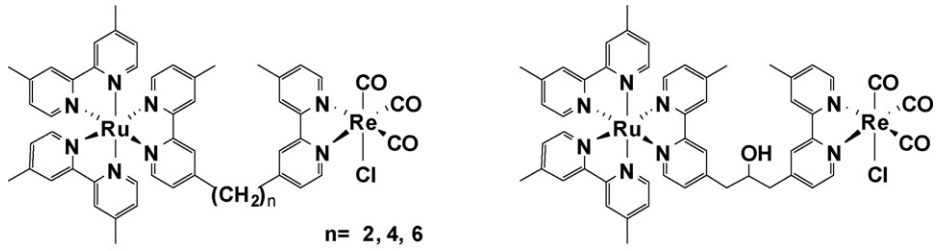

RuCnRe **RuC3(OH)Re**

Scheme 1.

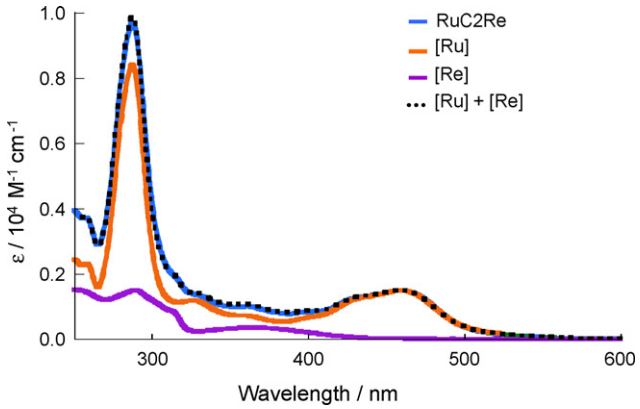

Fig. 1. UV–vis absorption spectra of **RuC2Re**, $[Ru(dmb)_3]^{2+}$ (**[Ru]**), *fac*-$Re(dmb)(CO)_3Cl$ (**[Re]**), and the 1:1 summation spectrum of **[Ru]** and **[Re]** (dotted line). The solvent was MeCN.

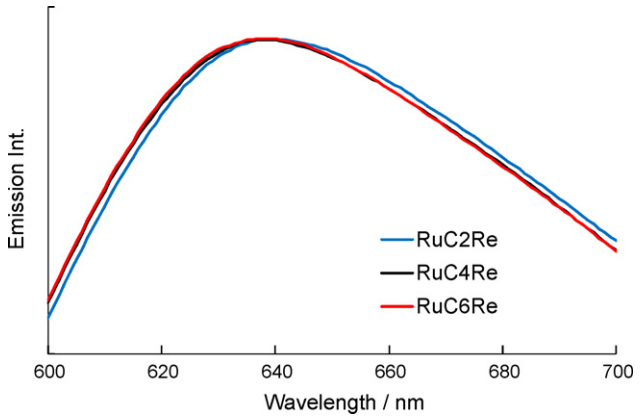

Fig. 2. Emission spectra of the diads measured at 25 °C in DMF. The excitation wavelength was 480 nm.

absorption of the Re(I) site and the Ru(II) site, respectively. The strong absorption band at around 290 nm is attributed to the π–π^* absorption of the diimine ligands on both Re(I) and Ru(II).

On the other hand, a small difference in emission spectra was observed between **RuC2Re** and the other diads. As shown in Fig. 2, all the diads emitted from the ^{3}MLCT excited state of the Ru(II) site at around 640 nm. Although both the shape and quantum yield (Table 1) of the emission were similar, the emission spectrum of **RuC2Re** was 2-nm red-shifted when compared with those of **RuC4Re** and **RuC6Re** (Fig. 2). The lifetimes of emission of the Ru(II) sites were almost identical for all of the diads (Table 1).

Table 1
Photophysical properties of the diads.

Complex	λ_{abs} (ε)[a] (nm, 10^3 mol^{-1} cm^{-1})	λ_{em}[b] (nm)	Φ_{em}[b]	τ[b] (ns)
RuC2Re	287 (98.1), 459 (14.9)	640	0.057	916
RuC4Re	287 (98.8), 459 (15.0)	638	0.058	915
RuC6Re	287 (96.8), 459 (14.9)	638	0.059	910
$[Ru(dmb)_3]^{2+}$	287 (84.0), 459 (14.9)	638	0.058	881

[a] Measured in MeCN.
[b] Mesured in DMF.

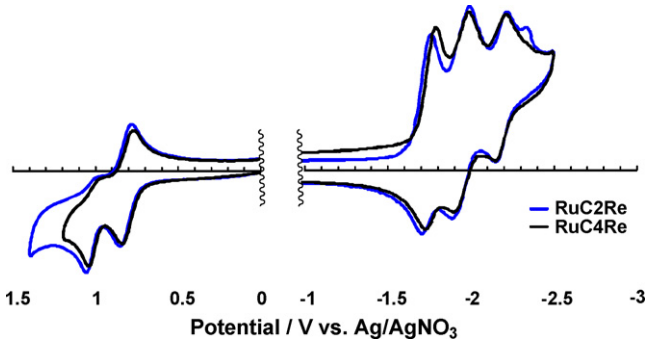

Fig. 3. Cyclic voltammograms of **RuC2Re** and **RuC4Re** measured in MeCN containing Et_4NBF_4 as a supporting electrolyte.

2.2. Electrochemical properties

Fig. 3 illustrates the cyclic voltammograms (CV) of the diads measured in MeCN containing Et_4NBF_4 as a supporting electrolyte. The first reversible and second irreversible oxidation waves are attributable to Ru(II/III) and Re(I/II) in the diads, respectively, because of the similarity with those of the corresponding mononuclear complexes as summarized in Table 2. In the reduction site,

Table 2
Redox potentials of the diads and their model complexes.

Complex	$E(\Delta E)$[a] (V) vs. $Ag/AgNO_3$ (mV)			
	$Re^{I/II}$	$Ru^{II/III}$	$Re(L/L^{\bullet-})$	$Ru(L/L^{\bullet-})$
RuC2Re	1.05	0.82 (70)	−1.72 (64)	−1.72 (64), −1.93 (109), −2.18 (77)
RuC4Re	1.04	0.80 (75)	−1.75 (65)	−1.75 (65), −1.93 (124), −2.17 (86)
RuC6Re	1.04	0.80 (75)	−1.75 (83)	−1.75 (83), −1.94 (119), −2.18 (82)
$[Ru(dmb)_3]^{2+}$	–	0.80 (70)	–	−1.77 (60), −1.96 (60), −2.22 (70)
fac-$Re(dmb)(CO)_3Cl$	0.99	–	−1.77 (65)	–

[a] Measured in MeCN solutions containing Et_4NBF_4 (0.1 M) with the scan rate of 200 mV s^{-1}.

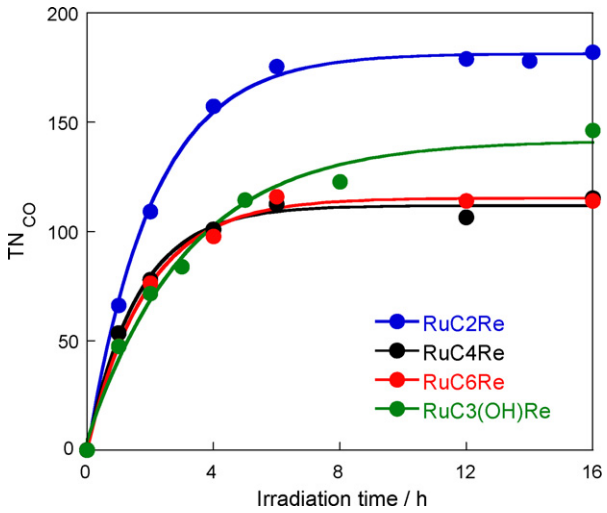

Fig. 4. Turnover number for CO formation from CO_2 as a function of irradiation time. Solutions were irradiated using a high-pressure Hg lamp with filters producing <500-nm light. The concentration of the diads was 0.05 mM in a CO_2-saturated DMF-TEOA (5:1) solution containing 0.1 M of BNAH. Data for **RuC3(OH)Re** are from reference [8].

the first reversible wave at $E^{red}_{1/2} = \sim -1.75$ V corresponds to two-electron reduction and is attributed to the reduction of both the bridge ligand on the Re site and one of the diimine ligands on the Ru site. The corresponding Re(I) and Ru(II) mononuclear complexes were also reduced at very similar potentials (Table 2). The other reduction waves observed at more negative potentials are assigned to reduction of the other diimine ligands on Ru and Re (0/+), which overlapped at $E^{red}_{p} = -1.95$ V.

Although the electrochemical behaviors of the diads were almost identical to the combination of those of the corresponding Ru(II) and Re(I) mononuclear complexes, we detected small differences between **RuC2Re** and the other diads; both the first oxidation and the first reduction waves of **RuC2Re** were observed at more positive potentials by 20–30 mV (Fig. 3; Table 2). This result indicates that there is a very weak interaction between the Ru(II) and Re(I) sites in **RuC2Re**, but not in **RuC4Re** and **RuC6Re**. This intramolecular interaction should be the origin of the difference of emission maxima between **RuC2Re** and the other diads, as described in Section 2.1.

2.3. Photocatalytic reactions

In a typical run, a 5:1 dimethylformamide (DMF)–triethanolamine (TEOA) solution containing a diad (0.05×10^{-3} M) and 1-benzyl-1,4-dihydronicotinamide (BNAH, 0.1 M) as the reductant, was irradiated under a CO_2 atmosphere using >500-nm light. The photocatalytic formation of CO, along with very small amounts of H_2, was observed using all of the diads. Formic acid was not detected in any of the cases. Fig. 4 shows the turnover numbers (TN_{CO}, mol of CO produced/mol of the complex used) as a function of irradiation time, when **RuC3(OH)Re** is also added [8]. The most efficient photocatalyst is **RuC2Re**, for which a quantum yield (Φ_{CO}) of 0.13 was determined using 546-nm monochromic light (light intensity: 4.916×10^{-6} einstein min^{-1}) and for which the TN_{CO} was about 180. On the other hand, the photocatalyses of **RuC4Re** and **RuC6Re** were almost identical to each other ($\Phi_{CO} = 0.11$, $TN_{CO} = 115$), and they were both of lower when compared to **RuC2Re**. It is noteworthy that the photocatalysis by **RuC4Re** and **RuC6Re** was similar to that of **RuC3(OH)Re**.

The UV–vis absorption spectra of the diads and the corresponding mononuclear complexes in Fig. 1 clearly indicate that the ^{3}MLCT excited state of the Ru site on all of the diad is selectively produced in the first stage of the photocatalytic reaction by irradiation using > 500-nm light. This is also supported by the fact that the shape and strength of the emission from the diad were very similar to those from **$[Ru(dmb)_3]^{2+}$** (Fig. 2; Table 1).

Emission from the excited state of the Ru site was selectively quenched by BNAH, but not by TEOA, which functions as a base. Fig. 5 shows the Stern–Volmer plots for the quenching of emission from the diads with BNAH, all of which demonstrated good linearities.

This should be reductive quenching; e.g., the photocatalytic reactions should be initiated by electron transfer from BNAH to the ^{3}MLCT excited state of the Ru site in the diads (Eq. (1)) because of the similarity of the photophysical and electrochemical properties of **RuC3(OH)Re** and the diads reported here [7,8].

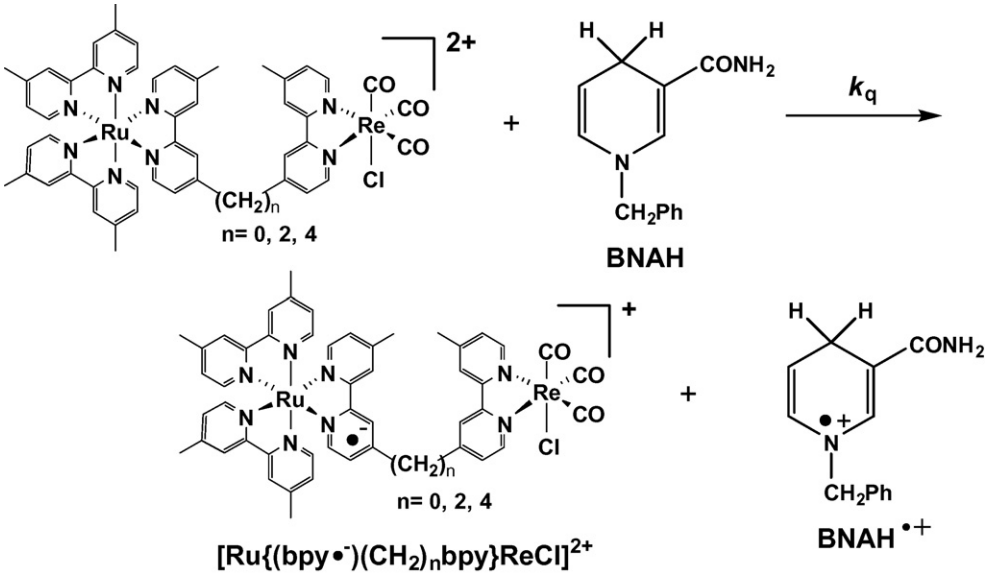

(1)

Fig. 5 clearly indicates that the quenching for the ^{3}MLCT excited state of **RuC2Re** is obviously more efficient than those for **RuC4Re** and **RuC6Re**, which were very similar to each other. The quenching rate constants are summarized in Table 3. Emission from two mononuclear Ru(II) complexes, $[Ru(dmb)_3]^{2+}$ and $[Ru(dmb)_2(\eta^2\text{-MebpyC}_2H_4\text{Mebpy})]^{2+}$ where a diimine function on one side of the $(Mebpy)C_2H_4(Mebpy)$ ligand coordinates to Ru(II) and another diimine function on the other side is free for coordination, was

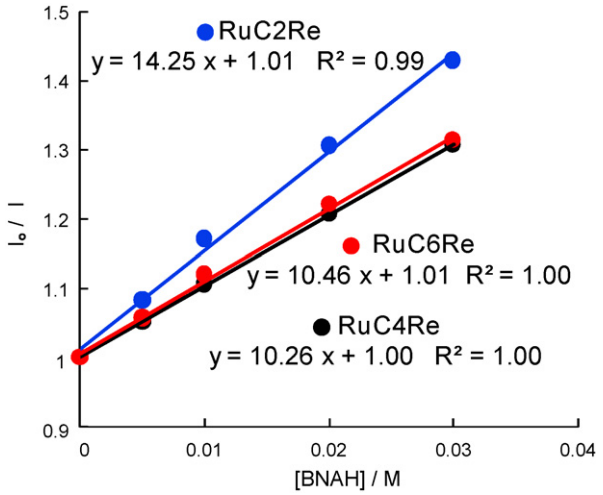

Fig. 5. Stern–Volmer plots the quenching of emission from the diads with BNAH. Excitation and detection wavelength were 530 and 640 nm, respectively. The solvent was DMF-TEOA (5:1, v/v).

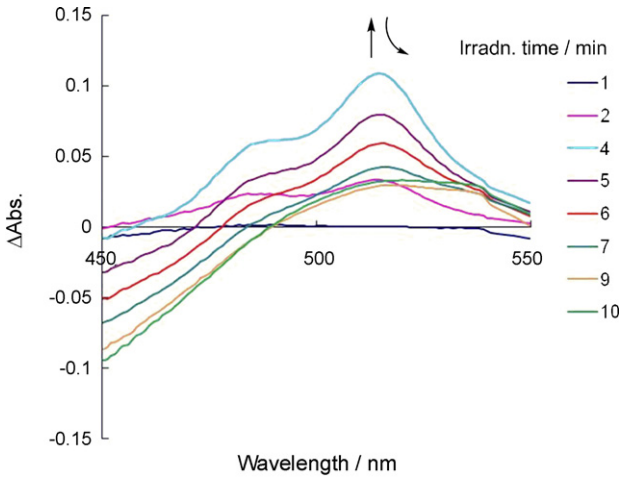

Fig. 6. UV–vis absorption spectral changes of the photocatalytic reaction solution using **RuC2Re**.

Table 3
Photocatalytic reactions using RuCnRe.

Complex	Φ_{CO}	TN	k_q (10^7 M^{-1} s^{-1})	$100\eta_p$ (%)	Φ_{CO}/η_p
RuC2Re	0.13	180	1.53	58	0.22
RuC4Re	0.11	120	1.09	50	0.22
RuC6Re	0.11	120	1.10	50	0.22

also quenched with $k_q\tau = 12.0$ and 12.1 M^{-1}, respectively. These values are smaller than that for **RuC2Re** ($k_q\tau = 14.3$), but larger than those for **RuC4Re** and **RuC6Re** ($k_q\tau = 10.3$, 10.5 M^{-1}). These results also indicate an interaction between Ru and Re through the (Mebpy)C_2H_4(Mebpy) ligand; i.e., in **RuC2Re**, it is weak but obviously exists. On the other hand, the other bridge ligands cannot give any through-bond interaction between the two metal centers. Since the lifetime of emission from **RuC2Re** was almost identical with the other diads (Table 1), the more efficient quenching for the ^{3}MLCT of **RuC2Re** compared with the others should mainly attributed to the higher oxidation power of the Ru site caused by the weak interaction with the Re site (see Section 2.2).[1]

We can calculate quenching fractions (η_q) of emission from the diads with BNAH (0.1 M) under photocatalytic condition using the values $k_q\tau$[BNAH] and Eq. (2) (Table 3).

$$\eta_q = \frac{k_q\tau[\mathrm{BNAH}]}{1 + k_q\tau[\mathrm{BNAH}]} \quad (2)$$

[1] The slower quenching in the cases of **RuC4Re** and **RuC6Re** compared with mononuclear Ru(II) complexes possibly caused by the steric hindrance by the Re site.

The quenching fraction should affect the efficiency of the photocatalysis of the diad because the reductive quenching is the first process of the photocatalytic reaction (Eq. (1)). Table 3 also shows the values of Φ_{CO}/η_q. The similarity of Φ_{CO}/η_q among the three diads clearly indicates that the higher photocatalytic ability of **RuC2Re** is mainly caused by the faster quenching rate of its ^{3}MLCT with BNAH. The electron transfer rate from the Ru site to the Re site (Eq. (3)) might be another factor, but it could play only a minor role because it is not a rate-determining process in the photocatalytic reaction.

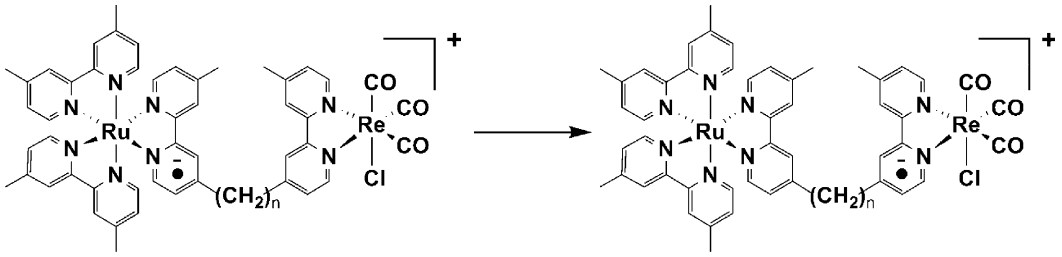

$$[Ru\{(Mebpy^{\cdot-})(CH_2)_nMebpy\}Re]^+ \rightarrow [Ru\{Mebpy(CH_2)_n(Mebpy^{\cdot-})\}Re]^+ \quad (3)$$

Fig. 6 shows the UV–vis absorption spectral change of the photocatalytic reaction solution using **RuC2Re**. In the first stage of the photocatalytic reaction, new absorption peaks appear at 480–550 nm with vibrational structure, which is a typical absorption for one-electron reduced (OER) species of Re diimine complexes, such as [Re^I(dmb^-)$(CO)_3${P$(OEt)_3$}] [2c,8]. Therefore, electron transfer from the Ru site to the Re site should efficiently occur (Eq. (3)). Further irradiation causes a decrease of the absorption, but CO continues to be produced. Similar phenomena have been reported in cases using not only Ru–Re diad systems [7,8] but also mononuclear Re complexes [1b,5]. This is attributed to loss of the Cl^- ligand from the OER species to produce a coordinately unsaturated species that should react with CO_2 to furnish a CO_2 adduct. Some free Cl^- may recoordinate to the Re (I) in the diad after CO_2 reduction occurs, but other diad molecules should have DMF or TEOA as ligands instead of Cl^-, which can also function as a photocatalyst for CO_2 reduction [5,8]. Although we cannot identify the structure of the CO_2 adduct or the source of the second electron transferred to it, there are two possible mechanisms: (1) the Ru site in the CO_2 adduct again functions as a photosensitizer and/or (2) another OER species [5] or coordinately unsaturated complex reacts with the CO_2 adduct [9].

3. Experimental

3.1. General procedures

UV–vis absorption spectra were measured with a JASCO V-565 spectrophotometer. Proton-NMR spectra were measured in an acetone-d_6 solution using a JEOL AL300 (300 MHz) or AL400 (400 MHz) system. The residual protons of acetone-d_6 were used as an internal standard for the measurements. Electrospray ionization time-of-flight mass spectroscopy (ESI-TOFMS) was performed with a Waters LCT Premier with methanol as the mobile phase.

Emission spectra were recorded with a JASCO FP-6500 spectrofluorometer, and were corrected for detection sensitivity using correction data supplied from JASCO. Emission quantum yields were evaluated with $Ru(bpy)_3^{2+}$ ($\Phi_{em} = 0.062$) in degassed acetonitrile as the standard [10]. Emission lifetimes of the metal complexes were measured with a Horiba NAES-1100 time-correlated single-photon counting system (the excitation source was an NFL-111 nanosecond H_2 lamp, and the instrument response was less than 1 ns). The samples were degassed by the freeze-pump-thaw method before the measurements. Emission quenching experiments were made on Ar-saturated solutions containing 5 different concentrations of the quencher BNAH. Values of k_q were calculated from linear Stern–Volmer plots for the luminescence of the ^{3}MLCT excited state of the Ru site and knowledge of its lifetime.

The redox potentials of the complexes were measured in an acetonitrile solution containing tetraethylammonium tetrafluoroborate (0.1 M) as a supporting electrolyte by cyclic voltammetric techniques, using an ALS/CHI CHI-620 electrochemical analyzer with a glassy-carbon disk working electrode (3 mm diameter), a $Ag/AgNO_3$ (0.01 M) reference electrode, and a Pt counter electrode. The supporting electrolyte was dried in a vacuum at 100 °C for 1 day prior to use. The scan rate was 200 mV s^{-1}.

3.2. Photocatalytic reactions

Photocatalytic reactions were performed in 11.4×10^{-3} dm^3 test tubes (i.d. = 8 mm) containing a 4×10^{-3} dm^3 DMF/TEOA (5:1, v/v) solution of the metal complexes (0.05×10^{-3} mol dm^{-3}) and BNAH (0.1 mol dm^{-3}), following purging with CO_2 for 20 min. For selective excitation of the ruthenium moiety, the solution was irradiated in a merry-go-round irradiation apparatus at $\lambda \geq 500$ nm using a high-pressure Hg lamp combined with a uranyl glass and a K_2CrO_4 (30%, w/w, $d = 1$ cm) solution filter. During irradiation, the tube was cooled with tap water. For the quantum yield measurements, we used a quartz cubic cell with an Ushio Optical Modulex high-pressure Hg lamp BA-H500 combined with a 546-nm (FWHM = 10 nm) band pass filter, purchased from Asahi Spectra Co., and a 5-cm long $CuSO_4$ solution (250 g/L) filter. The temperatures of the solutions were controlled at 25 ± 0.2 °C using a TAITEC Lab-Bath LB-21JR cooling thermo pump during irradiation. The incident light intensity was determined using a $K_3Fe(C_2O_4)_3$ actinometer [11]. The gaseous reaction products, i.e., CO and H_2, were analyzed by GC-TCD (GL science GC323).

3.3. Materials

Acetonitrile was distilled over P_2O_5 and then over CaH_2. DMF was dried over molecular sieves (4A) and distilled under reduced pressure (2.6 kPa). Triethanolamine (TEOA) was distilled under reduced pressure (4.0×10^{-2} kPa). All of the purified solvents were kept under Ar until use. Hydrated ruthenium trichloride was purchased from Kojima Chemical Co. and was used as received. All other reagents were reagent-grade quality and were used without further purification.

3.4. Synthesis

1-Benzyl-1,4-dihydronicotineamide (BNAH) [12], the bridge ligands $Mebpy(CH_2)_nMebpy$ [13], and $Ru(Me_2bpy)_2Cl_2$ (Me_2bpy = 4,4′-dimethyl-2,2′-bipyridine) [14] were prepared as according to the literature.

$[(Me_2bpy)_2Ru(MebpyC_2H_4Mebpy)](PF_6)_2$: To a solution of $MebpyC_2H_4Mebpy$ (190 mg, 0.519 mmol) in 10 mL of MeOH was added $(Me_2bpy)_2RuCl_2$ (100 mg, 0.173 mmol), and the mixture was heated at reflux for 12 h under N_2 in the dark. The solvent was evaporated, the residue was dissolved in water, and $MebpyC_2Mebpy$ was precipitated as a white solids and was filtered out. After the water was evaporated, the complex was isolated by column chromatography on alumina using a mixture of MeCN, methylenechloride, and methanol as eluents, followed by the addition of a saturated aqueous NH_4PF_6 solution. The product was precipitated as the PF_6^- salt from the concentrate by the addition of water and then filtered and recrystallized from methanol. Yield: 55%. ^{1}H NMR (400 MHz; $(CD_3)_2CO$): δ 8.78 (s, 1H, α-py-3), 8.64 (s, 5H, β-py-3, dmb-3,3′), 8.50 (d, 1H, J = 5.2, γ-py-6), 8.44 (d, 1H, J = 5.2, δ-py-6), 8.30 (s, 1H, γ-py-3), 8.29 (s, 1H, δ-py-3), 7.86 (d, 1H, J = 6.0, α-py-6), 7.82–7.79 (m, 4H, dmb-6,6′), 7.67 (d, 1H, J = 5.6, β-py-6), 7.46 (m, 1H, α-py-5), 7.34–7.37 (m, 4H, dmb-5,5′), 7.21–7.27 (m, 3H, β-py-5, γ-py-5, δ-py-5), 3.15–3.30 (m, 4H, $-CH_2CH_2-$), 2.53 (m, 15H, β-py-CH_3, dmb-CH_3), 2.43 (s, 3H, δ-py-CH_3) ppm. ESI-MS (MeOH): m/z = 418 (M^{2+}).

The other mononuclear complexes with a bridge ligands were obtained in a similar manner to **$[(Me_2bpy)_2Ru(MebpyC_2H_4Mebpy)](PF_6)_2$**, using $MebpyC_4H_8Mebpy$ or $MebpyC_6H_{12}Mebpy$ instead of $MebpyC_2H_4Mebpy$.

$[(Me_2bpy)_2Ru(MebpyC_4H_8Mebpy)](PF_6)_2$: Yield: 35%. ^{1}H NMR (400 MHz; $(CD_3)_2CO$): δ 8.69 (s, 1H, α-py-3), 8.65 (s, 5H, β-py-3, dmb-3,3′), 8.50 (d, 1H, J = 4.9, γ-py-6), 8.44 (d, 1H, J = 5.1, δ-py-6), 8.29 (s, 1H, γ-py-3), 8.26 (s, 1H, δ-py-3), 7.86–7.77 (m, 6H, α-py-6, β-py-6, dmb-6,6′), 7.42 (d, 1H, J = 5.7, α-py-5), 7.37 (d, 4H, J = 5.7, dmb-5,5′), 7.32 (d, 1H, J = 6.5, β-py-5), 7.22 (m, 2H, γ-py-5, δ-py-5), 2.8 (m, 4H, α-py-CH_2-, γ-py-CH_2-, overlapped with the peak of water contained in the solvent), 2.54 (s, 3H, β-py-CH_3), 2.53 (s, 12H, dmb-CH_3), 2.43 (s, 3H, δ-py-CH_3), 1.79 (m, 4H, $-CH_2CH_2-$) ppm. ESI-MS (MeOH): m/z = 432 (M^{2+}).

$[(Me_2bpy)_2Ru(MebpyC_6H_{12}Mebpy)](PF_6)_2$: Yield: 40%. ^{1}H NMR (400 MHz; $(CD_3)_2CO$): δ 8.69 (s, 1H, α-py-3), 8.65 (s, 5H, β-py-3, dmb-3,3′), 8.51 (d, 1H, J = 4.9, γ-py-6), 8.47 (d, 1H, J = 5.0, δ-py-6), 8.30 (s, 1H, γ-py-3), 8.25 (s, 1H, δ-py-3), 7.88–7.78 (m, 6H, α-py-6, β-py-6, dmb-6,6′), 7.42 (d, 1H, J = 5.9, α-py-5) 7.37–7.32 (m, 5H, β-py-5, dmb-5,5′), 7.23–7.20 (m, 2H, γ-py-5, δ-py-5), 2.7 (m, 4H, α-py-CH_2-, γ-py-CH_2-, overlapped with the peak of water contained in the solvent), 2.54–2.53 (m, 15H, β-py-CH_3, dmb-CH_3), 2.43 (s, 3H, δ-py-CH_3), 1.70 (m, 4H, $-CH_2-$, $-CH_2-$), 1.43 (m, 4H, $-CH_2CH_2-$) ppm. ESI-MS (MeOH): m/z = 446 (M^{2+}).

[RuC2Re]$(PF_6)_2$: A methylenechloride solution containing 100 mg of **$[(Me_2bpy)_2Ru(MebpyC_2H_4Mebpy)](PF_6)_2$** (0.089 mmol) and 35.4 mg of $Re(CO)_5Cl$ (0.098 mmol) was refluxed under an Ar atmosphere for 3 h, and then the solvent was evaporated under reduced pressure. The residue was dissolved in methylenechloride, and diethylether was added to precipitate unreacted $Re(CO)_5Cl$, which was removed by filtration. After the solvent was removed, the residual solid was recrystallized from a mixed solution of methanol, acetone, and methylenechloride. Yield: 90%. ^{1}H NMR (400 MHz; $(CD_3)_2CO$): δ 8.92–8.83 (m, 2H, γ-py-6, δ-py-6), 8.69–8.47 (m, 8H, α-py-3, β-py-3, γ-py-3, δ-py-3, dmb-3,3′), 7.85–7.24 (m, 14H, α-py-6, β-py-6, dmb-6,6′, α-py-5, β-py-5, γ-py-5, δ-py-5, dmb-5,5′), 3.42–3.31 (m, 4H, -CH_2CH_2-), 2.61–2.47 (m, 18H, dmb-CH_3, β-py-CH_3, δ-py-CH_3) ppm. IR (in MeCN): ν_{CO} (cm^{-1}) 2022, 1915, 1897. ESI-TOFMS (m/z, eluent:MeOH): calcd for $C_{51}H_{46}ClF_{12}N_8O_3P_2ReRu$ (M^{2+}) 571.0992; found 571.0980.

The other dinuclear complexes were obtained in a similar manner to **[RuC2Re]**$(PF_6)_2$, using the corresponding mononuclear complex.

[RuC4Re]$(PF_6)_2$: Yield: 60%. ^{1}H NMR (400 MHz; $(CD_3)_2CO$): δ 8.91 (m, 2H, γ-py-6, δ-py-6), 8.67 (m, 2H, α-py-3, β-py-3), 8.64 (s, 4H, dmb-3,3′), 8.57–8.52 (m, 2H, γ-py-3, δ-py-3), 7.83–7.75 (m, 6H, dmb-6,6′, α-py-6, β-py-6), 7.60–7.55 (m, 2H, γ-py-5, δ-py-5), 7.37–7.32 (m, 6H, α-py-5, β-py-5, dmb-5,5′), 2.82 (m, 4H, α-py-CH_2-, γ-py-CH_2-), 2.53–2.58 (m, 18H, dmb-CH_3, β-py-CH_3, δ-bpy-CH_3), 1.85 (m, 4H, –CH_2CH_2–) ppm. IR (in MeCN): ν_{CO} (cm^{-1}) 2022, 1915, 1897. ESI-TOFMS (*m*/*z*, eluent:MeOH): calcd for $C_{53}H_{50}ClF_{12}N_8O_3P_2ReRu$ (M^{2+}) 585.1149; found 585.1141.

[RuC6Re]$(PF_6)_2$: Yield: 75%. ^{1}H NMR (400 MHz; $(CD_3)_2CO$): δ 8.90 (m, 2H, γ-py-6, δ-py-6), 8.67 (m, 2H, α-py-3, β-py-3), 8.64 (s, 4H, dmb-3,3′), 8.55 (m, 2H, γ-py-3, δ-py-3), 7.84–7.75 (m, 6H, dmb-6,6′, α-py-6, β-py-6), 7.60–7.54 (m, 2H, γ-py-5, δ-py-5), 7.39–7.35 (m, 6H, α-py-5, β-py-5, dmb-5,5′), 2.82 (m, 4H, α-py-CH_2-, γ-py-CH_2-), 2.53–2.59 (m, 18H, dmb-CH_3, β-py-CH_3, δ-py-CH_3), 1.77 (m, 4H, –CH_2–, –CH_2–), 1.43 (m, 4H, –CH_2CH_2–) ppm. IR (in MeCN): ν_{CO} (cm^{-1}) 2021, 1915, 1897. ESI-TOFMS (*m*/*z*, eluent:MeOH): calcd for $C_{55}H_{54}ClF_{12}N_8O_3P_2ReRu$ (M^{2+}) 599.1306; found 599.1296.

4. Conclusion

We synthesized new Ru(II)-Re(I) diads to serve as CO_2 reduction photocatalysts, where two diimine ligands coordinating to Ru(II) and Re(I) metals are connected with different length of alkyl chains. The most efficient photocatalyst has the –C_2H_4– chain (**RuC2Re**), but no difference in photocatalysis was observed between the diads with –C_4H_8– (**RuC4Re**) and –C_6H_{12}– chains (**RuC6Re**), which were also close to the diad with a –$CH_2CH(OH)CH_2$– chain (**RuC3(OH)Re**), which was previously reported. Weak interaction between the Ru and Re sites was observed only in **RuC2Re**, but not in the other diads. This causes a higher reductive quenching efficiency of the ^{3}MLCT excited state of **RuC2Re** by the BNAH which leads to an increased quantum yield of CO_2 reduction.

References

[1] (a) J. Hawecker, J.-M. Lehn, R. Ziessel, J. Chem. Soc., Chem. Commun. (1984) 328–330;
(b) J. Hawecker, J.-M. Lehn, R. Ziessel, Helv. Chim. Acta 69 (1986) 1990–2012.
[2] (a) O. Ishitani, M.W. George, T. Ibusuki, P.A. Johnson, K. Koike, K. Nozaki, C. Pac, J.J. Turner, J.R. Westwell, Inorg. Chem. 33 (1994) 4712–4717;
(b) H. Hori, F.P.A. Johnson, K. Koike, K. Takeuchi, T. Ibusuki, O. Ishitani, J. Chem. Soc., Dalton Trans. (1997) 1019–1023;
(c) H. Hori, J. Ishihara, K. Koike, K. Takeuchi, T. Ibusuki, O. Ishitani, J. Photochem. Photobiol., A: Chem. 120 (1999) 119–124.
[3] (a) H. Hori, F.P.A. Johnson, K. Koike, O. Ishitani, T. Ibusuki, J. Photochem. Photobiol., A: Chem. 96 (1996) 171–174;
(b) K. Koike, H. Hori, M. Ishizuka, J.R. Westwell, K. Takeuchi, T. Ibusuki, K. Enjouji, H. Konno, K. Sakamoto, O. Ishitani, Organometallics 16 (1997) 5724–5729.
[4] (a) H. Tsubaki, A. Sekine, Y. Ohashi, K. Koike, H. Takeda, O. Ishitani, J. Am. Chem. Soc. 127 (2005) 15544–15555;
(b) H. Tsubaki, A. Sugawara, H. Takeda, B. Gholamkhass, K. Koike, O. Ishitani, Res. Chem. Intermed. 33 (2007) 37–48.
[5] H. Takeda, K. Koike, H. Inoue, O. Ishitani, J. Am. Chem. Soc. 130 (2008) 2023–2031.
[6] P. Kurz, B. Probst, B. Spingler, R. Alberto, Eur. J. Inorg. Chem. 15 (2006) 2966–2974.
[7] B. Gholamkhass, H. Mamaetuka, K. Koike, T. Tanabe, M. Furue, O. Ishitani, Inorg. Chem. 44 (2005) 2326–2336.
[8] S. Sato, K. Koike, H. Inoue, O. Ishitani, Photochem. Photobiol. Sci. 6 (2007) 454–461.
[9] Y. Hayashi, S. Kita, B.S. Brunschwig, E. Fujita, J. Am. Chem. Soc. 125 (2003) 11976–11987.
[10] J.V. Casper, T.J. Meyer, J. Am. Chem. Soc. 105 (1983) 5583–5590.
[11] C.G. Hatchard, C.A. Paker, Proc. R. Soc. Lond., Ser. A 235 (1956) 518–536.
[12] D. Mauzerall, F.H. Westheimer, J. Am. Chem. Soc. 77 (1955) 2261–2264.
[13] S. Ferrere, C.M. Elliott, Inorg. Chem. 34 (1995) 5818–5824.
[14] B.P. Sullivan, D.J. Salmon, T.J. Meyer, Inorg. Chem. 17 (1978) 3334–3341.